Nanoengineering of non-aqueous liquid electrolyte solutions for future lithium-metal batteries

Dominik Weintz[a], Martin Werres[b,c], Birger Horstmann[b,c], Rachid Amine[d*], Chi-Cheung Su[e], Xinlin Li[e], Yaobin Xu[f], Ridwan A. Ahmed[f], Wu Xu[f], Chongmin Wang[g], Bastian von Holtum[h], Simon Wiemers-Meyer[h], Dongliang Chen[i], Jianwei Lai[i], Feifei Shi[i], Sascha Berg[a], Egbert Figgemeier[a], Christian O. P. Rivera[j], Daniel Wang[k], Yang Shao-Horn[j,k,l], Aravind Unni[m], Ulrike Krewer[m], Stephen Scoggins[n], Perla B. Balbuena[n,o,p] , Jorge M. Seminario[n,o,q], Asia Sarycheva[r], Ziyuan Lyu[c,s], Dominic Bresser[c,s], Florian Hausen[t,u], Rüdiger-A. Eichel[t,u], Khalil Amine[d], Arnulf Latz[b,c**], Robert Kostecki[r**], Martin Winter[a,h] & Isidora Cekic-Laskovic[a*]

[a] *Forschungszentrum Jülich GmbH, Helmholtz-Institute Münster (IMD-4), Corrensstraße 48, 48149 Münster, Germany*

[b] *German Aerospace Center (DLR), Institute of Engineering Thermodynamics, Pfaffenwaldring 38-40, 70569 Stuttgart, Germany*

[c] *Helmholtz Institute Ulm for Electrochemical Energy Storage (HIU), Helmholtzstraße 11, 89081 Ulm, Germany*

[d] *Materials Science Division, Argonne National Laboratory, Lemont, Illinois 60439, USA*

[e] *Chemical Sciences and Engineering Division, Argonne National Laboratory, Lemont, Illinois 60439, USA*

[f] *Energy and Environment Directorate, Pacific Northwest National Laboratory, Richland, WA 99354, USA*

[g] *Environmental Molecular Sciences Laboratory, Pacific Northwest National Laboratory, Richland, WA 99354, USA*

[h] *University of Muenster, MEET Battery Research Center, Corrensstraße 46, 48149 Münster, Germany*

[i] *Department of Energy and Mineral Engineering and Materials Science and Engineering, The Pennsylvania State University, University Park, PA 16802, USA*

[j] *Department of Materials Science and Engineering, Massachusetts Institute of Technology, Cambridge, MA, 02139, USA*

[k] *Department of Mechanical Engineering, Massachusetts Institute of Technology, Cambridge, MA, 02139, USA*

[l] *Research Laboratory of Electronics, Massachusetts Institute of Technology, Cambridge, MA 02139, USA*

[m] *Institute for Applied Materials — Electrochemical Technologies, Karlsruhe Institute of Technology, 76131 Karlsruhe, Germany*

[n] *Department of Chemical Engineering, Texas A&M University, College Station, Texas 77843, USA*

[o] *Department of Materials Science and Engineering, Texas A&M University, College Station, TX, 77843, USA*

[p] *Department of Chemistry, Texas A&M University, College Station, TX, 77843, USA*

[q] *Department of Electrical Engineering, Texas A&M University, College Station, TX, 77843, USA*

[r] *Energy Storage and Distributed Resources Division, Lawrence Berkeley National Laboratory, Berkeley, California 94720, USA*

[s] *Karlsruhe Institute of Technology (KIT), P.O. Box 3640, 76021 Karlsruhe, Germany*

[t] *Institute of Energy Technologies (IET-1), Forschungszentrum Jülich GmbH, 52425 Jülich, Germany*

[u] *RWTH Aachen University, Institute of Physical Chemistry, Landoltweg 2, 52074 Aachen*

Corresponding authors: i.cekic-laskovic@fz-juelich.de; aminer@anl.gov;
Co-corresponding authors: Arnulf.Latz@dlr.de; r_kostecki@lbl.gov

Abstract

The increasing use of portable devices and the electrification of transportation have driven efforts to develop long-lasting, energy-dense methods for storing electrical energy alongside the state-of-the-art lithium ion battery technology. Lithium metal is a promising negative electrode of choice due to its high specific theoretical capacity of 3.86 Ah g^{-1} and 2.06 Ah cm^{-3}, which, in combination with lithium's very low redox potential (-3.04 *vs.* RHE), enables battery setups with unmatched energy density. The challenge, however, is to find a non-aqueous electrolyte formulation that enables reversible electrochemical stripping/plating of lithium metal in a dense and uniform fashion while protecting the alkali-metal electrode surface from degradation and favoring an effective interaction with other battery components. This review presents relevant electrolyte design approaches and discusses their application for the development of high-energy density non-aqueous lithium metal batteries (LMBs). Insights from latest research on lithium passivation and electrolyte properties are used to understand the formation kinetics of solid electrolyte interphase components at the nanoscale and uncover structure-property relationships. Building on these insights, potential research directions are explored, and an iterative electrolyte development process, utilizing modern machine learning as well as high-throughput computation and experimentation, is proposed to expedite electrolyte development for practical LMBs.

Introduction

The growing demand for portable electronic devices and the transition to electric transportation have driven efforts to enhance current lithium ion battery (LIB) technology, aiming for higher energy density and longer lifespans. Metallic lithium has emerged as a promising anode alternative due to its unmatched combination of high-specific capacity and low redox potential.[1,2] However, the safety concerns and the short cycle life of lithium metal batteries (LMBs) have limited its widespread use as an electrode material.[3,4] The challenge is to develop a suitable electrolyte that enables the reversible deposition and release of Li in a compact and uniform manner while protecting it from degradation and still being compatible with other battery components. The formation, composition and structure of the protective layer between the anode and the electrolyte, solid electrolyte interphase (SEI), are crucial parameters determining the performance and cycle life of an LMB.[5,6] In contrast to Li^+ host materials like graphite, common organic carbonate-based electrolytes fail to effectively protect metallic Li, since formed ineffective organic-rich SEI causes an inhomogeneous Li deposition and continuous interphase growth. This results in a cascade of failure mechanisms, including an accelerated electrolyte and Li consumption, the formation of electrochemically isolated "dead" Li and internal impedance growth.[4,7] High-performing liquid electrolytes for LMBs ideally form a homogeneous inorganic-rich SEI with fast self-healing kinetics, which can adapt to the high mechanical stress during galvanostatic cycling and promote compact Li deposits.[8,9] The capability of a liquid electrolyte to form an effective SEI is largely determined by the Li solvation sheath and binding strengths between each component. While cyclic carbonates like ethylene carbonate (EC) tend to interact strongly with the solvated Li^+, weakly binding solvents and high conducting salt concentrations (>>1 M) lead to the formation of contact-ion pairs (CIPs) and aggregates (AGGs), where the anion actively participates in the inner Li solvation shell. This promotes the reduction of the anion rather than the solvent and leads to a favorable inorganic-rich protection layer. Consequently, most high-performing liquid electrolytes widely adopt this solvation design strategy for LMBs[10]. However, further improvements are required to achieve a comparable performance to current LIBs.

This review discusses the thermodynamic and kinetic properties of liquid electrolytes, highlighting in particular the effects of high Li salt concentrations and solvation strength on the Li solvation shell and key electrolyte properties. These insights are analyzed regarding their effects on the SEI and with the latest discoveries about the performance-determining interphase, an ideal Li passivation is proposed. Furthermore, novel electrolyte concepts and design strategies to approach the ideal electrolyte and SEI-forming conditions are emphasized. Finally, recently utilized analytical tools and optimization potentials of the most promising electrolyte concepts are discussed and future design directions evaluated.

History of lithium-metal batteries

The development and rising popularity of portable electronic devices, and the invention of the implantable pacemaker in the 1950s and 60s, sparked the search for novel battery chemistries and led to the development of the first primary LMB by coupling a lithium metal anode with an iodine-polyvinyl pyridine cathode material achieving an at that time unprecedented energy density of ~250 Wh kg^{-1} (Figure 1).[11] Concurrently, the stability of lithium in non-aqueous electrolyte solutions and proposed protection mechanisms have

been explored, culminating in Peled's introduction of the SEI model in 1979.[12–14] Many companies wanted to use this knowledge and embarked on the quest to develop a rechargeable secondary LMB with a liquid electrolyte, which proved to be even more challenging than expected. During that time, several conducting salt-solvent combinations were investigated, some of which were either too dangerous or too toxic (e.g. $LiClO_4$ and $LiAsF_6$) or exhibited poor Li plating/stripping reversibility (e.g. organic carbonate-based electrolytes). Eventually, ethers like tetrahydrofuran (THF) and its derivatives became the solvent of choice due to their high stability against Li metal and low viscosity.[15] With that knowledge, MoLi Energy seemed to succeed in commercializing the technology with the Li intercalation material MoS_2 as cathode and an electrolyte composed of a Li salt in a mixture of several organic solvents. However, the safety tests performed were insufficient, resulting in numerous flame-related incidents that quickly led to the technology's decline.[3] The discovery of Li intercalation anode materials with a low potential vs. $Li|Li^+$ led to the commercialization of the LIB as we know it today and a drastic decline in efforts towards the further development of rechargeable LMBs in the late 80ies/early 90s.[14] In the mid-2000s, the need for high-energy density batteries led to the revival of the LMB, the exploration of new liquid electrolyte concepts and the utilization of film-forming additives to protect the lithium metal anode.[1,8]

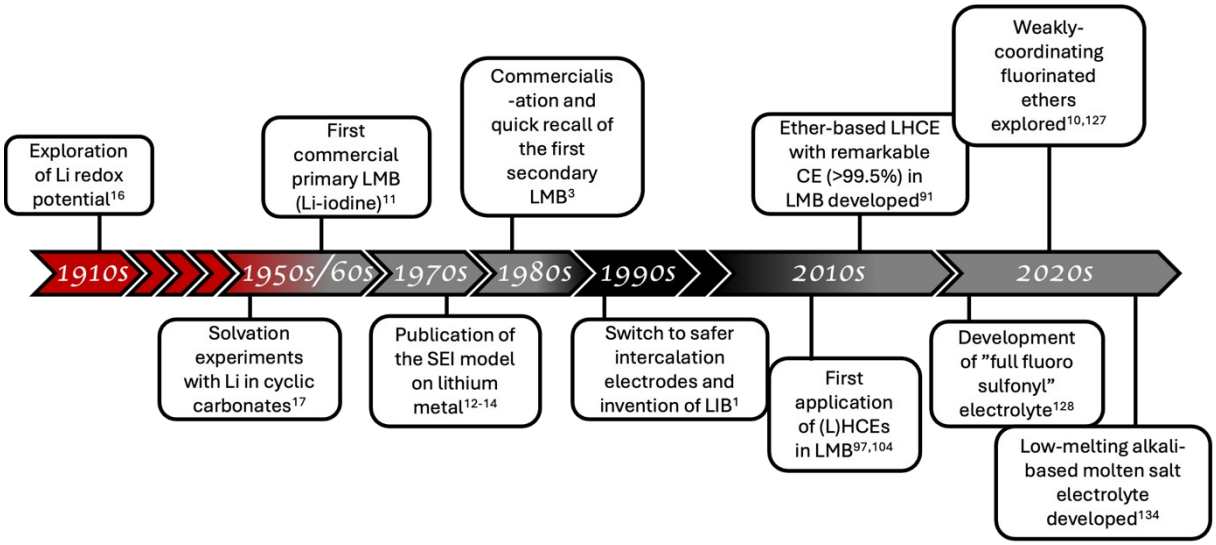

Figure 1: Historical milestones towards the development of a lithium metal battery.

Properties of liquid electrolytes

Intrinsic physical & chemical properties

The solvation environment of Li has a great impact on the dynamics of the electrolyte including the transport, interface kinetics and thermodynamic properties. Traditional metrics like the dielectric constant and donor number (DN) are used to evaluate solvent-ion interactions, providing a macroscopic view of a solvent's ability to dissociate salts and solvate ions and being the basis for designing novel electrolyte formulations.[19]

The electrochemical stability window (ESW) is another critical parameter for electrolyte stability evaluation, defined as the voltage range between their reduction and oxidation limits. To roughly estimate the ESW, molecular orbital-based analysis is commonly used by assessing the energy gap between the highest occupied molecular orbital (HOMO) and the lowest unoccupied molecular orbital (LUMO) of the solvent[20]. However, this isolated-molecule-based evaluation occasionally deviates from experimental ESW, as usually strong ion interactions in the electrolyte can impact the HOMO/LUMO considerably.[21] Despite their simplicity, HOMO/LUMO values still provide easy-to-obtain rough estimations and often align with the reduction/oxidation limits of corresponding electrolytes.

Transport kinetic properties

Ionic conductivity is a key transport property of electrolytes, reflecting how freely ions move to participate in electrochemical reactions, thereby significantly influencing a battery's power output and the Li deposition morphology at higher current densities.
Since the reactions at the electrodes in LMBs depend on the Li^+ transport, it is crucial to quantify the Li^+ contribution to overall ionic conductivity. The two critical transport properties here are the transport number (t) and the transference number (T).[22] Although often used interchangeably, they are fundamentally different: the transport number quantifies the relative mobility of each ionic species (e.g., Li^+ and $[Li_2X]^+$), whereas the transference number measures the net transference of all Li^+-containing species. In most organic solvent-based electrolytes the Li^+ transference number is more relevant to battery chemistry and usually hovers ≈0.3, indicating that most current is carried by anions.[23,24] Despite extensive research, accurately determining the transference number remains challenging, unlike ionic conductivity determination, for which well-established measurement methods exist.[25–27]

Thermodynamic properties

Although dielectric constant and DN are commonly used to assess solvation strength, they do not fully capture the complex ion-ion and ion-dipole interactions in common lithium-based electrolytes. These usually contain a combination of free solvents, solvent-separated ion pairs (SSIPs) as well as CIPs, and AGGs, where the anions actively participate in the solvation of Li^+. To understand electrolyte solvation structures, it's crucial to quantify the Gibbs free energy, entropy, and enthalpy changes of ion-pair solvation, reflecting the competition and equilibrium among ionic species.[28] These crucial thermodynamic metrics are rarely reported for battery electrolytes, and their fundamental correlation with battery performance remains largely unexplored. Understanding these macroscopic thermodynamic properties is essential for linking them to the microscopic ion-pairing dynamics, where $Li^+ \leftrightarrow$ anion association occurs concurrently with $Li^+ \leftrightarrow$ solvent dissociation.

Interface phenomena

A step beyond the analysis of bulk electrolytes is defined by interfacial simulations. A recent study combines classical molecular dynamics (MD), tight binding simulations and density functional theory (DFT) calculations to investigate how multicomponent liquid

electrolytes react within the electrical double layer (EDL) and give predictions of potential reduction products. The results indicate that for anions to effectively participate in SEI formation, they must be present in the EDL and the lithium solvation sheath (CIP or AGG).[29] Additional outcomes of interfacial simulations are given by the first principles-based analysis of changes in solvation structures and their effects on (de-)solvation barriers at interfaces. By analyzing cation diffusion, desolvation and deposition pathways for different liquid electrolytes, researchers can gain new insights into the potential transport and electrodeposition barriers from a given electrolyte in the vicinity of the electrode surface. These barriers arise from the competition between solvation forces and solvent electron affinity toward the electrode surface.[30]

Impact of solvent & salt concentration

Two major solvent groups have been identified for Li-based electrolytes, each offering an adequate combination of essential physicochemical, electrochemical and thermal properties. Cyclic organic carbonates (e.g. EC), common in commercially available LIBs, have comparably high viscosities, high oxidative stability and strong interactions with the dissolved Li^+. Ethers (e.g. THF, 1,2-dimethoxyethane (DME)) on the other hand generally exhibit lower viscosities and higher reductive stability, thus providing a better Li metal compatibility compared to cyclic carbonates.[8,31]

In recent years, high-concentration electrolytes (HCEs) have been intensively investigated, especially for use in LMBs. Increased conducting salt concentration from 1-1.2 M to 4-6 M results in a shift from the SSIPs-dominated solvation structure, commonly found in moderate concentration electrolytes (MCEs), to CIPs and AGGs, with strong ion-ion and solvent-ion interactions.[32] This results in a change of several vital electrolyte properties: 1) Due to the stronger solvent-ion interactions, the ESW widens, increasing the stability of the solvent against reduction, which promotes a favorable and effective anion-derived inorganic SEI.[33] 2) The widened EWS increases the oxidative stability of the solvent, making even oxidative fragile ethers like DME usable with most 4 V cathode chemistries.[34] 3) Beyond a certain conducting salt concentration threshold, the transport properties of the ions change fundamentally. Instead of the usually observed ion transport via the “vehicle-type” mechanism based on diffusion, a Li^+ hopping mechanism has been proposed and experimentally proven in certain HCEs, where the solvating moieties of the solvent and anion bridge different Li^+, thereby enabling the hopping between different Li coordination sites.[35] Even though the increase in viscosity reduces the overall ionic conductivity, the high conducting salt concentration prevents rapid depletion of the Li^+ near the interface and enable homogeneous Li plating even at high current densities.[33] Another approach to favor the formation of CIPs and AGGs is using weakly solvating solvents, such as fluorinated 1,2-diethoxyethane (DEE) derivates and steric demanding solvents, which promote the formation of favorable anion-derived interphases even at moderate concentrations of 1-1.2 M.[10,36] Electrolytes containing weakly coordinating ethers and HCEs have high energy barriers to ion movement near the anode surface. In this case, the anions have a high electron affinity towards the Li metal, which leads to rapid deposition of inorganic SEI products on the surface.[32] However, this also causes the weak solvation strength to be inversely proportional to the ion mobility; therefore, a balance still needs to be found to enable sufficient power density of the battery (Figure 2b).[10] Ultimately, since salt is the primary cost driver of liquid electrolytes, using HCEs always raises material costs.

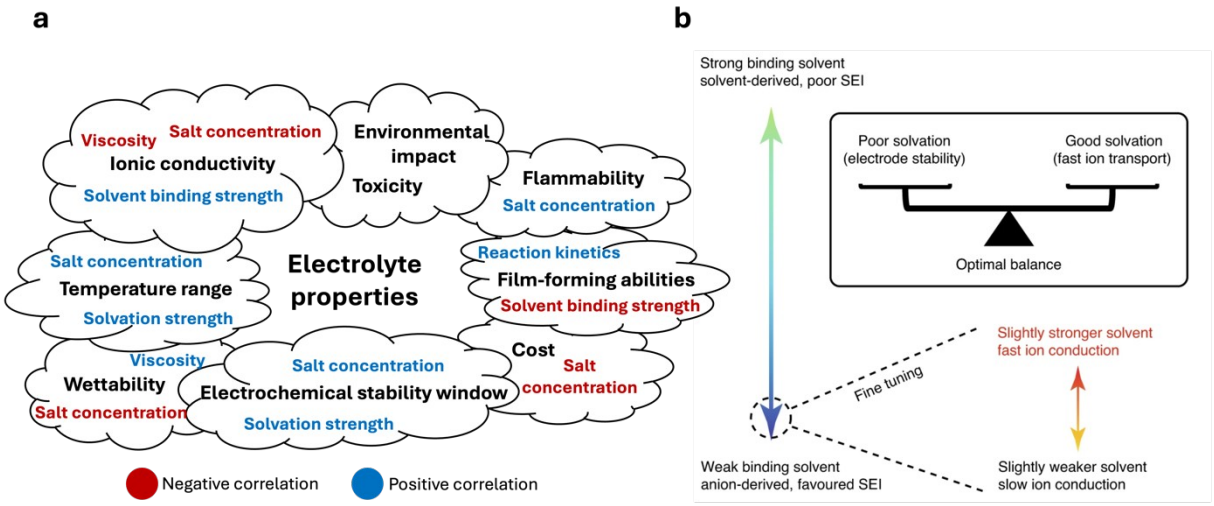

Figure 2: a) Electrolyte properties and impact factors b) Anti-correlation between film-forming abilities and ionic conductivity based on the solvent solvation strength.

Solid Electrolyte Interphase

The SEI, which ideally acts as protective layer against further decomposition reactions, usually consists of fully reduced inorganic species near the Li metal and organic species in the outer SEI, often arranged in a mosaic-like structure. However, several reports state the formation of amorphous and multilayer interphases with certain electrolyte formulations and galvanostatic cycling conditions.[5] Nucleation and growth of the SEI are mostly based on an electron tunneling model with a self-limiting thickness of 2-3 nm, which deviates from the experimentally determined values ranging from 6 to 50 nm.[37–41] The mechanism for further growth beyond the critical tunneling thickness[37,42] remains elusive; however, several mechanisms were proposed for further SEI growth[43], i.e., electron diffusion through point defects like Li interstitials[44,45], solvent diffusion[46,47], electron conduction through SEI layer[46–48] , and transition metal-enabled electron transfer, whereby the transition metals stem from the cathode and deposit on the anode[49]. For excess-free LMBs, the SEI forms on copper (Cu) during the first cycle before Li deposition occurs, whereas, for LMBs with Li reservoirs, the Li metal comes with a native passivation layer (NPL) that forms during inevitable atmosphere exposure.[50,51] This native layer, mainly composed of Li_2CO_3, LiOH and Li_2O dictates the SEI formation and composition upon electrolyte contact. Even after several cycles, its effect on the SEI, Li deposition morphology and relevant performance parameters is still pronounced.[52,53] Similarly, imperfections of the Cu current collector, including microcracks and oxide layer formation result in heterogeneous Li deposits.[54,55] Besides the influence of the anode and current collector surface, several other parameters can impact the SEI properties, including the electrolyte formulation (i.e., salt anion[56], solvent[57], and additive[58]), current density, operating voltage, counter electrode[59], pressure, and temperature[60,61]. The SEI properties determine the morphology and mechanism of the metal deposition and dissolution process as well as the anode corrosion rate.[62]

Mechanical properties

During charge/discharge, the substantial volume changes of the Li metal electrode can cause cracks in the SEI, exposing reactive Li to the electrolyte, highlighting the importance of the SEI's mechanical properties in LMBs. The ideal mechanical properties of the SEI are, however, seemingly contradicting: For two-dimensional plating, a high elastic modulus is desirable, while to mitigate cracking, a flexible SEI is desirable, which can also be achieved by high mechanical strength and high ductility.[2,63] Several research groups have investigated the elastic modulus of the SEI formed in different electrolytes, with values ranging from 0.3 GPa for organic carbonate-based formulations up to over 5 GPa in HCEs and ether-based electrolytes.[41,64] Simulations and experimental data indicate that elastic moduli of over 3 GPa result in good SEI stability and elastic modulus exceeding that of Li (4.9 to 7.8 GPa) have been shown to partially suppress the formation of Li whiskers.[64–66] Recent studies by Gao et al. propose that optimizing the elastic modulus and elastic strain limit, essentially maximizing the elastic deformation energy, is key to further enhancing the Coulombic efficiency (CE), suggesting a multilayer interphase layer which incorporates both inorganic and organic as the ideal SEI structure.[67–69]

Ionic and electronic transport properties

Understanding the SEI requires knowledge of electronic and ionic conduction mechanisms. Their investigation is, however, rather difficult due to the ultrathin and sensitive nature of the SEI and the lack of appropriate instruments/techniques. Excess interstitial Li^+ has been identified as a possible carrier in the inorganic layer transported via a knock-off mechanism through the crystal inorganic lattice and mesoscale modeling revealed that diffusion in the SEI follows the structural layered pattern, switching from knock-off to pore diffusion in the outer layer.[70,71] By applying a newly established *in situ* liquid secondary ion mass spectroscopy (SIMS) technique combined with transmission electron microscopy (TEM) on an isotope-labeled SEI, Zhu et al. experimentally proved that Li^+ transport follows a mechanism of successive displacement, rather than a “direct-hopping” in the SEI. They further revealed that the Li^+ self-diffusion varies, with higher diffusivity ($6.7 \cdot 10$-19 m^2 s^{-1}) in the outer carbon-enriched SEI and lower diffusivity ($1.0 \cdot 10^{-20}$ m^2 s-1) in the inner carbon-depleted SEI, providing a quantitative gauging of ionic behavior of SEI layer against the underlining electrode.[72] Consistent with these results, others have focused on demonstrating ion transport through SEI grain boundaries, which suggests the importance of understanding the nanoscale growth of the SEI and the formation of specific crystal interfaces.[73,74] Recently, Xu et al. developed an *in situ* biasing TEM method for directly measuring the electrical properties of SEI layers. Contrary to previous assumptions, the SEI layers exhibit semiconducting rather than electronically insulating behavior, supporting the theoretical simulations by Köbbing *et al.* and Balbuena, Seminario *et al.*, who observed similar conductance in their calculations.[75–78] Furthermore, the high proportion of organic components in the SEI will cause large porosity, the presence of charged molecular fragments or organic radical species and the existence of large amounts of dissolved Li ions, which may lead to the formation of electrochemically inactive “dead” Li.[75] Here, metallic Li remnants remain unstripped in the SEI shell and are electronically isolated from the current collector and Li anode. Similar to ion conduction, grain boundaries between SEI compounds have been predicted to also enhance electron transport in the SEI.[79] Since the inner layer of the SEI is a composite structure with crystalline particles (including organic and inorganic species)

dispersed in the amorphous matrix, the electron leakage and ion transport properties are determined by the continuous amorphous matrix rather than the dispersed crystalline particles.

Lithium deposition morphology

A major cause of the short cycle life and the origin of safety hazards is the Li deposition morphology, as inhomogeneous Li deposits increase the surface area, necessitating more decomposition reactions.[2] The Li deposition morphology can be distinguished in favorable compact low surface area deposits and high surface area lithium (HSAL) morphologies, such as Li whiskers, mossy Li deposition and Li dendrites, which are linked to a low CE due to the increase in reaction sides and their significant contribution towards the formation of "dead" Li.[80,81] Typically, dendrites only arise above the limiting current density after Sand's time due to a depletion of ions near the electrode and are thereby limited by the electrolyte and ion mobility.[82] On the other hand, mossy Li and Li whiskers arise from an ineffective SEI formation.[83,84] The electric properties are of high importance as the deposited Li particles exhibit a wide size distribution, large fractions of "dead" Li and a high topographical tortuosity at high rates of differential conductions.[75] Of equal importance is the homogeneity of the protecting SEI layer to enable uniform Li plating, as slight inhomogeneities and cracks can lead to Li whisker formation as a result of local stress and current hotspots.[85] Several studies correlated the charge-transfer and SEI formation kinetics with the Li deposition morphology, assuming that fast kinetics or self-healing rates promote compact Li deposition morphology.[9,86,87] Recent mesoscale kinetic Monte Carlo (kMC) simulation further revealed that clogging of the grain boundaries due to extensive SEI growth causes spatial variations and kinetic limitations of the Li transport, promoting the growth of Li whiskers and heterogeneous Li deposits.[88,89]

Optimizing the SEI layer to achieve ideal electronic resistance, ionic conductivity, mechanical strength, and flexibility may seem contradictory. LiF is widely regarded as one of the holy grail SEI components due to its very high mechanical strength and electronic resistance, leading to many past research efforts to solely increase the LiF content.[86,90,91] Given the complex nature and broad range of desired SEI properties, achieving effective Li protection with a compact deposition morphology may require more than simply increasing the LiF content as other inorganic Li components such as Li_2O have also been associated with a higher CE in LMBs, even without the presence of fluorine in the electrolyte.[92] Besides that, the presence of electronegative fluorine- and oxygen-rich functional groups has been shown to increase the SEI formation kinetics and, eventually, a faster and more homogeneous SEI repair.[9]

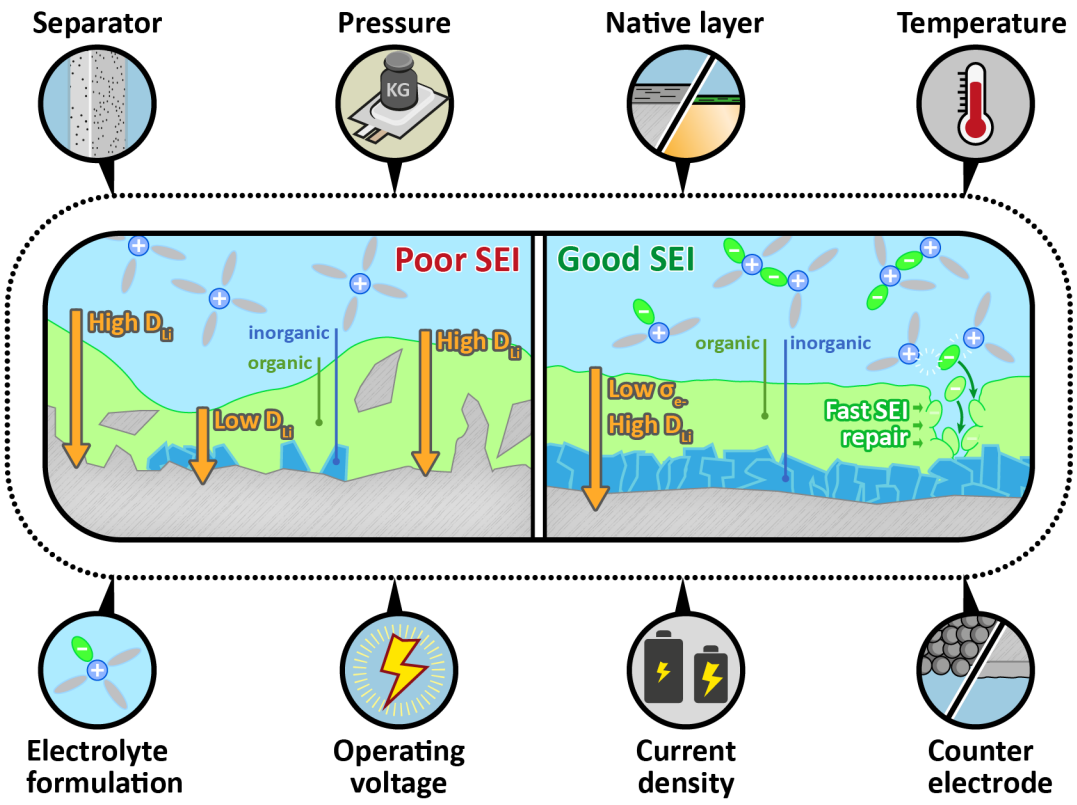

Figure 3: Comparison between a poorly protective SEI (left) and an effectively protective SEI layer (right), including the major impact factors during SEI formation.

This might be just the beginning of a more comprehensive understanding of the SEI non-metallic Li. With the advancement of analytical techniques and the predicting power of computational methods, a meaningful correlation between key SEI parameters can be achieved.

Liquid electrolytes for LMBs

The recently sparked interest in LMBs has led to a variety of newly developed liquid electrolytes to accommodate the harsh requirements of the Li metal anode. Several design strategies have been pursued, each taking a different approach to achieve the desired electrolyte and SEI properties.

Localized high-concentration electrolytes

HCEs are considered as promising alternatives to conventional MCEs for the further advancement of Li battery technologies.[93,94] However, the accompanying disadvantages

include high viscosity, low ionic conductivity, poor wettability of separators and thick electrodes, as well as high cost. Adding a non-solvating solvent (*i.e.* diluent) to an HCE so-called localized high-concentration electrolytes (LHCEs) are generated, which have shown noteworthy improvements to the electrochemical performance of LMBs compared to HCEs and organic carbonate-based MCEs.[95–97] LHCEs have substantially lower viscosity, enhanced wettability and reduced cost compared to their HCE counterparts.[7] As the favorable inner solvation sheath of Li^+, consisting of CIPs and AGGs, remains largely unchanged, most benefits of an HCE persist.[98,99] According to the design principle, an effective LHCE requires a diluent with low viscosity, none-to-low solvating capability of the conducting salt (DN ≤ 10) and sufficient miscibility with the solvating solvent.[100,101] Designing an ideal LHCE depends on the precise combination and quantity of the conducting salt, solvent and the appropriate diluent.[102] Since the first report on LHCEs, the electrolyte design strategy has achieved tremendous success in enhancing the electrochemical performance of various Li-based battery chemistries.[95,96,103–106] The unique structure of LHCEs fosters the formation of larger, more uniform, compact Li deposits, achieving higher CE than HCEs and MCEs.[104,107] A typical LHCE reported for LMBs in literature is lithium bis(fluorosulfonyl)imide (LiFSI) in DME diluted by 1,1,2,2-tetrafluoroethyl-2,2,3,3-tetrafluoropropyl ether (TTE) (1:1.2:3 by mol), which enables a high CE of 99.5%, yields compact, granular Li deposition and outperforms several LHCEs containing other solvating solvents and diluents.[95,108] Thus, it enables long-term cycling stability with a $LiNi_{0.6}Co_{0.2}Mn_{0.2}O_2$ (NMC622) electrode under practical conditions, i.e., over 600 cycles at 76 % capacity retention in a 2 Ah LMB with a specific energy of 350 Wh kg^{-1}.[109] Further studies have demonstrated that diluents with weak solvating capability in LHCEs enhance the LMB performance as such diluents can partially participate in the solvation structure, reduce the solvation strength of the solvent and contribute more to the formation of thin but robust electrode|electrolyte interphases.[110,111] Examples of such weakly coordinating diluents include bis(2,2,2-trifluorothyoxy)methane (BTFM)[112], 1,1,2,2-tetrafluoro-3-methoxypropane (TFMP)[113], 2,3-difluoroethoxybenzene (DFEB)[91], and 1,2-bis(1,1,2,2-tetrafluoroethoxy)ethane (BTFEE)[114,115]. Recent advances in LHCEs have also led to the development of electrolytes with unique structures and properties, further improving specific performance parameters of LMB.[116–119] To circumvent the poor high-rate performance, Kim *et al.* developed a high-entropy electrolyte by increasing the molecular diversity. This electrolyte, comprising five different solvents and diluents, doubled the ionic conductivity compared to the baseline LHCE by forming small solvation clusters, which improved high-rate performance at current densities >1 mA cm^{-2}.[120] Understanding the strong correlation between the solvation structure of LHCEs and their transport is crucial for advancing LHCEs and enhancing LMB performance.

Fluorinated carbonates & ethers

Besides the promising LHCEs, several novel MCEs have been investigated, mainly based on fluorinated derivates of well-known solvents. Fluorination commonly increases the oxidative stability, ensuring compatibility with high-voltage cathodes, while promoting an F-rich, inorganic SEI with increased formation kinetics.[121] Commercially available film-forming additives fluoroethylene carbonate (FEC) and difluoroethylene carbonate (DFEC) have proven to promote a compact Li deposition morphology. The replacement of EC with FEC/DFEC in 1M $LiPF_6$/EC/DMC and 1.2M $LiPF_6$/EC/EMC electrolytes demonstrated

improved capacity retention and high lithium stripping/plating efficiency of the resulting batteries.[122–124]

Another promising approach is the targeted fluorination of ethers. The molecular design principle focuses on judiciously manipulating the fluorination degree and relative positions to ethereal oxygens to reach the most appropriate tradeoff among oxidation/reduction stabilities, solvation strength, ionic conductivity and viscosity.[10,125] In DME and its derivates, the ether groups in the ethylene oxide segment solvate Li^+ through a five-member ring configuration, which offers good solubility and facilitates cation-anion separation. The targeted introduction of electron-withdrawing functional groups (-CF_3, -F) can modulate the electronic properties while retaining the favored five-member-ring solvation structure. For example, F5DEE, with a CHF_2 and CF_3 terminal group, and 1,1,1-trifluoro-2,3-dimethoxypropane (TFDMP) exhibits the optimum binding strength to the Li^+ promoting a high CE of 99.5% at low overpotential.[10,112] Several fluorinated mono-oxygen ethers have also been proposed as electrolyte solvents, with the symmetric difluorinated diethyl ether (BFE) enabling very efficient lithium plating/stripping with a high CE of 99.75%.[126]

Inorganic, liquified gas & full fluorosulfonyl electrolytes

Recently, Xue et al. developed the concept of full fluorosulfonyl (FFS) electrolytes by coupling LiFSI with an FSI-derived solvent DMTMSA ($FSO_2NC_2H_6$).[127–129] This novel electrolyte forms a highly robust LiF-enriched SEI and achieves an initial CE of ≈91%, rapidly increasing to ≈99% within just ten cycles. The high compatibility of FFS electrolytes with LMA can be attributed to the unique solvent properties. DFT calculations and experimental analyses indicate that FFS solvents have higher binding energy with Li than other film-forming solvents like FEC, promoting the formation of an inorganic-rich SEI that effectively suppresses dendritic growth and enhances the overall stability of the interphase layer. In addition, further “exotic” electrolyte designs include molten salt and liquified gas electrolytes. Fluoro- and difluoromethane have been successfully utilized as electrolyte solvents in pressure-controlled batteries containing achieving high average CEs of up to 99.6 % and showing promising results over an extensive temperature range (-60 to 60 °C).[130,131] More recently, Vu *et al.* reported a solvent-free inorganic molten-salt mixtures of alkali-based bis(fluorosulfonyl)amide salts to combine the nonvolatility and safety of solids with the interfacial stability and ionic conductivity of organic liquids.[132] Binary and ternary mixtures of $Li_{0.45}K_{0.55}FSI$ and $Li_{0.30}K_{0.35}Cs_{0.35}FSI$ have melting temperatures of 68 °C and 45 °C, respectively, ionic conductivities of ~1 mS cm^{-1} at 60 °C, high oxidative stability up to 6 V *vs.* $Li|Li^+$, and effectively passivate aluminum. These molten-salt mixtures led to compact Li deposition morphologies and an inorganic SEI layer with high CEs of up to 99.8 % and low overpotentials at 80 °C.[132]

Multi-salt electrolytes & film-forming additives

Several salt combinations and film-forming additives have been investigated to improve the electrochemical performance of LMBs. Notably, LiDFOB[133,134], $LiNO_3$[135,136] and various sulfonyl imides[135–138] were utilized in various blended salt electrolytes, showing synergistic effects during interphase formation. However, LiFSI remains the most promising conducting salt for LMB electrolytes due to its well-rounded properties and effective film-forming abilities. Among the countless additives that have been proposed for LMBs, fluorination agents (such as FEC[87,139] and DFEC[140]) as well as $LiNO_3$[135,141] proved to be highly

effective in promoting a favorable SEI composition and compact Li deposition. However, due to the constant reformation/repair of the SEI in LMBs during galvanostatic cycling, film-forming additives are consumed relatively quickly, diminishing their impact after several cycles.[139] In contrast, Ding et al. reported Cs-based salt as a non-sacrificial additive that promotes a homogeneous and compact Li deposition morphology due to the proposed electrostatic shield mechanism induced by Cs^+.[142]

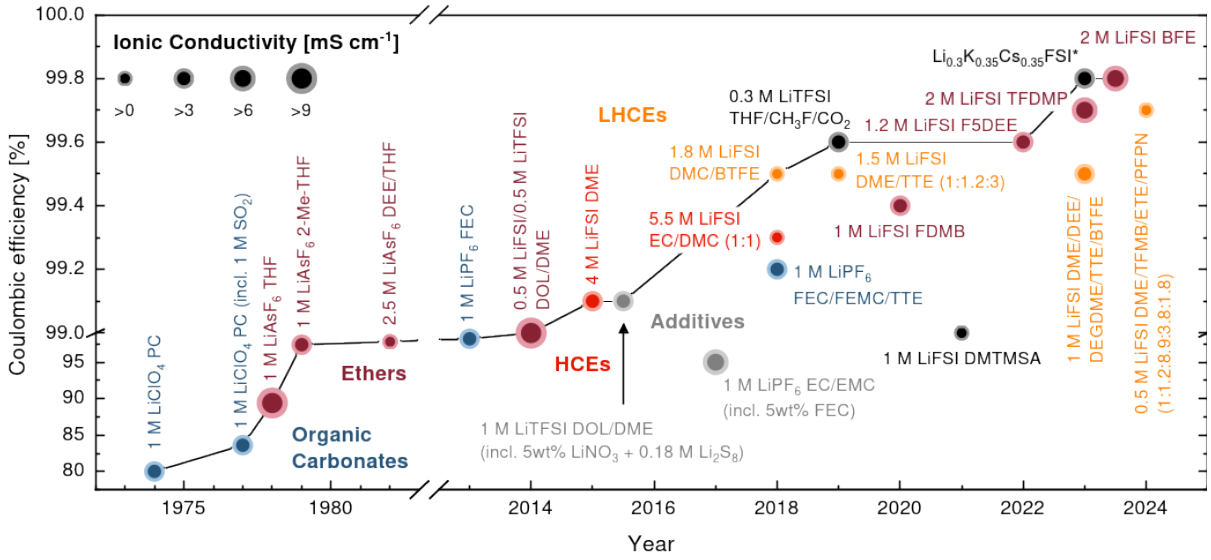

Figure 4: Evolution of high-performance liquid electrolytes and their Li stripping/plating efficiency (LilCu cell setup). DOL: 1,3-dioxolane, DMC: dimethyl carbonate, FDMB: 2,2,3,3-tetrafluoro-1,4-dimethoxylbutane, TFDMP: 1,1,1-trifluoro-2,3-dimethoxypropane, DEGDME: 2-Methoxyethyl ether, TFMB: trifluoromethoxybenzene, ETE: ethyl 1,1,2,2-tetrafluoroethyl ether, PFPN: ethoxy(pentafluoro)cyclotriphosphazene.
*Data collected at 80 °C

Analytical techniques

For the evaluation of designed LMB electrolytes and comparison to current state-of-the-art electrolytes, complementary analysis techniques, ranging from basic to advanced, are introduced to address the critical performance-determining parameters. The most common techniques are summarized in Table 1.

Property	Technique/Method	Setup/Tools
Solvation structure	Raman[143]	Raman spectrometer + sample carrier for liquids
	X-ray scattering[120,144]	Electrolyte sample is placed between X-ray beam and detector
	MD simulation[120]	Theoretical simulation based on calculated quantum data (i.e. DFT)
Ion mobility	Impedance spectroscopy[145]	Commercially available sensors, separator-free battery setup

	PFG-NMR[146], eNMR[26,146,147], Hittorf[23,24] and Bruce-Vincent method[148]	Different experimental setups depending on the method
Electrochemical stability window	Linear sweep voltammetry (LSV), Cyclic voltammetry (CV)[149]	Three-electrode battery setup (e.g. Swagelok™ or El-cell™)
Flammability	Self-extinguishing time (SET) determination[150]	Non-flammable electrolyte holder (e.g. glass fiber separator) + ignition source
Thermal stability	Differential scanning calorimetry (DSC)[151]	DCS device + electrolyte sample and reference
	Thermogravimetric analysis (TGA)[152]	TGA device + electrolyte sample

Table 1: Analysis techniques to investigate the bulk properties of electrolyte formulations for LMBs.

To evaluate the performance of LMB electrolytes, it is important to consider battery setups and conditions that meet the established battery community standards:

- Anode: Limited Li reservoir (<50 µm)
- Cathode: State-of-the-art materials with high-loadings (>3 mAh cm^{-2})
- Electrolyte: Limited electrolyte quantity (~2-3 g Ah^{-1})
- Cycling conditions: Application-oriented (>0.5 mA cm^{-2})

Electrochemical techniques

The Aurbach method employing a Li||Cu battery setup is considered the standard method for determining the CE and the Li loss per cycle, while long-term cycling provides valuable information about the CE evolution and cycle life.[153] Furthermore, the voltage profiles provide information on the internal resistance, and when coupled with electrochemical impedance spectroscopy (EIS), they provide information about the resistance contributions.[145] The key performance parameters include capacity retention, cycle life, voltage profiles, and battery polarization development. Additionally, the dQ/dV and dV/dQ plots extracted from voltage data offer valuable initial insights into the degradation origin, e.g. loss of (cathode) active materials, the increase in impedance and the loss of Li inventory.[154]

Interface & interphase characterization

Characterization of the electrode|electrolyte interfaces and formed interphases remains a challenging task. Understanding of the formation mechanisms and property relationships is still incomplete. This calls for characterization methods that allow analysis under *in situ* or *operando* conditions that closely mimic real-world scenarios.[155]

Microscopic level insights on SEI

The nanoscale structure of the SEI requires advanced analytical techniques with high spatial resolution. Scanning electron microscopy (SEM), as a powerful tool to investigate the Li deposition morphology, can provide detailed 2D/3D microstructural information, ranging from micrometer to nanometer scale. Recently, cryogenic transmission electron microscopy (TEM), has proven to be an effective method for revealing the structural

properties of the SEI layer with very high spatial resolution (down to atomic scale).[38,39] This method further assisted in solving many scientific questions related to the SEI, such as its nanostructure[38,39], current density effects[84], the relationship between the SEI and the Li morphology[156], battery operation temperature[157,158] and CE[92,125]. Furthermore, the advancement of high-speed detectors and novel imaging methods such as 4D-scanning TEM (4D-STEM) provide the chance to a more comprehensive picture of exotic physical properties of SEI, such as orientation of inorganic species, which may affect the ionic/electrical/mechanical properties of the SEI[79,159,160], strain field, electrical field and charge density distribution inside SEI[161,162]. Another technique often applied to study the morphology and mechanical properties of the SEI on various types of battery materials is electrochemical atomic force microscopy (EC-AFM), which allows operation under various conditions.[163–165]

Chemical distribution of the SEI

A wide range of analytical techniques is required to identify and quantify the inorganic and organic compounds in the SEI. However, the difficulty of analysis depends on the compound, as some require advanced sample treatment to enable the desired analysis, while others can be analyzed almost directly from the Li metal anode. Common identification of most inorganic compounds can be achieved by analyzing the electrodes *via* X-ray photoelectron spectroscopy (XPS)[52,166], X-ray diffraction (XRD)[167,168], ToF-SIMS[169], Fourier transform infrared (FTIR)[170], Raman[171] or nuclear magnetic resonance (NMR) spectroscopy[172], with ToF-SIMS, FTIR, Raman and NMR providing information on both inorganic and organic compounds. In addition, ^{7}Li NMR is a powerful technique to analyze morphological changes in the Li metal and quantify the formation of dead Li even *in situ*.[173,174] Identifying and quantifying organic SEI compounds is considered even more challenging than inorganic species. The detection of functional groups or repetitive structural motives, like -CO_3, C-O, C=O or C-H has been achieved in a number of publications by direct electrode analysis *via* XPS[52] or FTIR[170]. These techniques are limited in identifying or reconstructing entire molecular structures in the SEI, which necessitates the use of mass spectrometry .[169,175]

By combining microscopic analysis techniques with spectroscopy, spatial and chemical information can be investigated simultaneously. Energy dispersive spectroscopy (EDS) detectors are often integrated into SEMs, yielding information about the spatial elemental distribution.[176] Cryogenic STEM has also been successfully paired with electron energy loss spectroscopy (EELS) and EDS to obtain high-resolution structural and chemical information as well as the characterization of the electronic structure and bonding environment.[177,178] Besides EM techniques, atomic force microscopy (AFM) can be combined with IR spectroscopy to couple the morphological and mechanical information gained by AFM with chemical information about the interphase.[179,180]

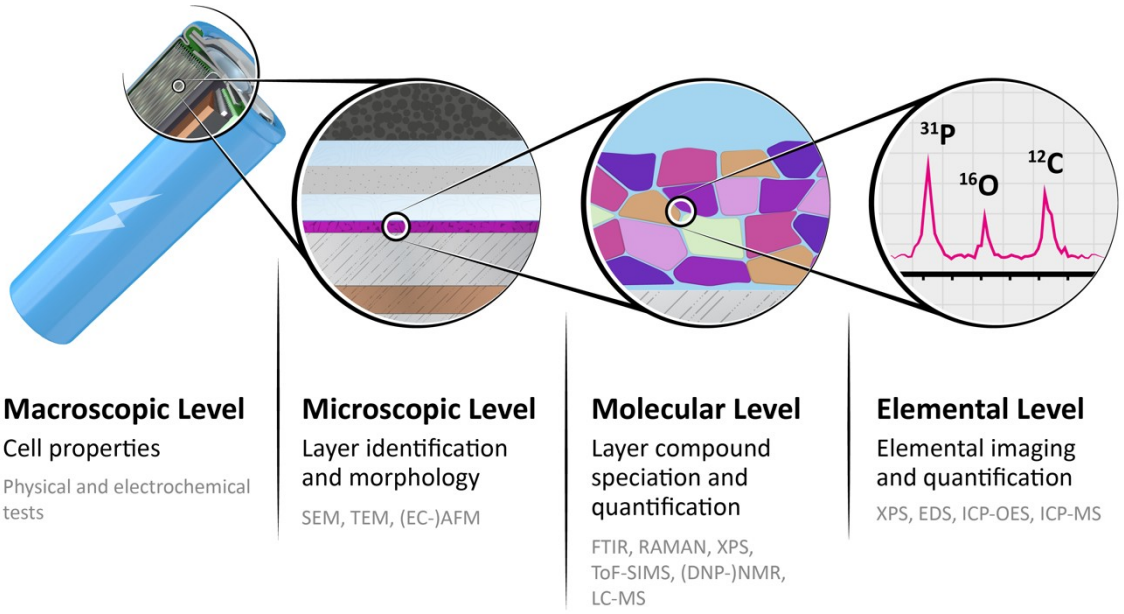

Figure 5: Overview of interphase characterization techniques.

Finally, multiscale modeling based on first-principle methods such as DFT and ab initio MD can provide a deeper understanding of the underlying interphase formation processes and decomposition reaction pathways.[166,181] Less computationally expensive *ab-initio* based mesoscale techniques (i.e. kMC) can capture the interphase dynamics over larger timescales (up to hours) and enable a direct correlation with experimental data.[89,182] To advance the understanding of the SEI and its complex nature, the combined use of complementary experimental and theoretical techniques is necessary to correlate structural and chemical information with other interphase layer properties. Further refinement and development of novel *in situ* and *operando* techniques with short measurement times enables investigation of the highly-dynamic electrochemical processes and further closes the gap between experimental data and simulations.

Conclusion and Perspective

The novel electrolyte concepts including systematic design of novel solvents/co-solvents resulted in considerably improved electrochemical performance of high-energy density LMBs, increasing the CE up to 99.7%. However, to enable practical zero-excess LMBs with cycle life rivaling current LIBs, the CE has to be in the vicinity of 99.95-99.98% (80% SOH after 450 to 1100 cycles), which is still a roughly tenfold improvement over today's best-performing liquid electrolytes. The main challenges remain in an effective Li protection with minimal losses of active material during cycling, making the SEI the most critical component in the LMB. Here, the latest research suggests aiming for fast SEI formation kinetics with homogeneously distributed inorganic-rich decomposition products like Li_3N, Li_2O, and LiF due to their high mechanical strength combined with good electrical insulating properties. The presence of polymer chains in the SEI's outer layer is also considered beneficial, increasing the flexibility and adaptability of the interphase layer to the mechanical stress during Li plating/stripping. Due to the brittle and air/moisture-sensitive nature of the SEI, the combined use of advanced *in situ* and *operando* analysis

techniques is required to investigate relevant formation processes and interphase properties. Here, further increasing the measurements temporal resolution is crucial to capture the short-lived intermediate species and fast SEI evolution mechanisms, as well as closing the gap to theoretical simulations, usually operating in narrow time frames. Similar to the SEI, a challenging and often anticorrelating set of requirements is necessary for liquid electrolytes to achieve an overall good battery performance, including a preferential rapid reductive decomposition of the anion by simultaneously achieving sufficient oxidative stability as well as a high ionic conductivity to avoid dendrite formation at higher current densities. A deeper understanding and optimization of Li^+ solvation, including the size and shape of the resulting clusters and binding strengths between each electrolyte component, are crucial as they determine most of the vital electrolyte properties. Simultaneously, industry-relevant electrolyte properties such as cost structure, safety, environmental impact, and temperature range should be considered, to determine if a novel electrolyte formulation can transition from lab to industry scale.

In recent years, different approaches have been pursued to unite the challenging requirements towards achieving high CEs under practical conditions. Additional exploration and design of novel electrolyte components, especially solvents, can help tune the solvation sheath for improved electrolyte properties and SEI formation. Starting from simple mono- and diether molecules, rational and systematic synthesis of derivates with electron-withdrawing or sterically demanding groups has already been shown to yield solvents, that enable very efficient Li plating/stripping. Further understanding of the structure-property relationships between the functional groups is essential to guide synthesis approaches and help fine-tuning the Li^+-solvent solvation strength and solvation clusters. Similar to the solvents, investigating the structure-property relationship between Li salts and SEI can guide rational anion design for desired SEI properties. Combining several different conducting salts and solvents can further help fine-tune the solvation structure, such as in the case of LHCEs in a synergistic fashion. Lastly, developing and utilizing novel functional additives is anticipated to further enhance the performance of liquid electrolytes. However, it is essential to understand the interaction of additives with other electrolyte components, their impact on other relevant electrolyte properties and their potential consumption rates.

The almost infinite number of possible small molecules combined with modern synthesis techniques provide nearly endless possibilities for the targeted design of novel electrolyte components. However, the synthesis and characterization of all possible candidates is a very intricate and time-intensive process, making a certain pre-selection process and rapid screening crucial to identify promising candidates. Here, three methods stand out which are gaining increasingly more attention: 1) HTE[183] allows for accelerating the experimental screening of promising electrolyte compositions. 2) High-throughput quantum mechanical (HTQM) calculations can calculate electrolyte properties or substitute for time-intensive experiments. 3) Machine learning (ML) enables predictions of electrolyte components/compositions based on a large database of internal and public experimental and simulation data. By analyzing and correlating large datasets of structural, electrolyte, and performance properties, ML allows us to explore the vast chemical landscape and to identify critical descriptors – mostly based on electrolyte properties – that have the greatest impact on a targeted performance

metrics.[184,185] The scope of the to-be-screened materials includes all possible molecules suitable as liquid electrolyte components, estimated to be in the vicinity of 10^{9-10}.

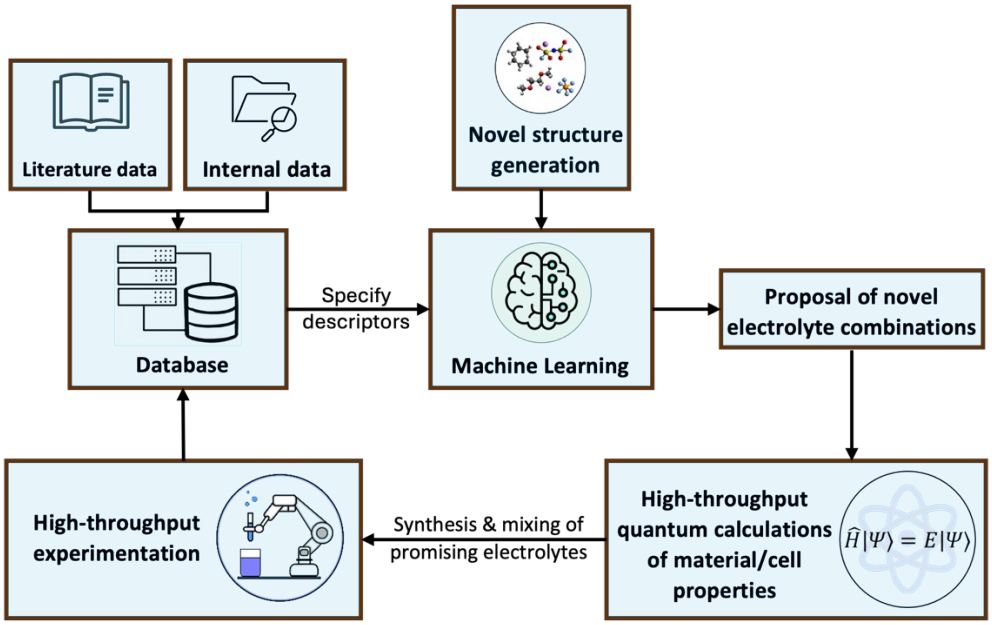

Figure 6: Iterative process scheme for an accelerated electrolyte development.

At present, most ML models focus on predicting the desired electrolyte property/performance metric based on other electrolyte properties. For the proposed electrolyte development process, an attribute-driven inverse design approach is preferred, where desired properties are the input and the model identifies suitable electrolytes (Figure 6).[186] In this approach, identifying better descriptors for a given target property, especially based on structural relations, is crucial to effectively screen the almost infinite number of possible electrolyte compositions. Subsequent HTQM calculations can help to pre-screen the proposed components proposed by the ML algorithm.[187–189] The QM data from the most promising candidates can further be used for more advanced simulations, giving estimates about bulk and dynamic electrolyte properties as well as insights into the SEI formation via *ab initio* methods[187]. Finally, after targeted synthesis and formulation of the best electrolyte candidates, HTE can be utilized to acquire desired datasets. Several HTE methods have already been increasingly adopted for electrolyte studies in recent years.[190–192] For example, HTE facilities were utilized to screen through 2002 samples, created by combining five additives from a pool of fourteen, to identify synergistic combinations that enhanced the CE of LMBs.[190]Furthermore, coupled HTE and ML analysis enables to optimize bulk ionic conductivity and identify the optimum electrolyte compositions for Li-based batteries.[191–194] Continuous refinement of ML models, methods, input data, standardized experimental protocols and open-source databases, will improve the ability to predict appropriate electrolyte formulations in a multi-institutional approach. This process is accelerated by more effective simulation methods and enhanced artificial intelligence capabilities of modern computer chips.

References

1. Hobold, G. M. *et al.* Moving beyond 99.9% Coulombic efficiency for lithium anodes in liquid electrolytes. *Nat. Energy* **6**, 951–960 (2021).
2. Horstmann, B. *et al.* Strategies towards enabling lithium metal in batteries: interphases and electrodes. *Energy Environ. Sci.* **14**, 5289–5314 (2021).
3. Brandt, K. & Laman, F. C. Reproducibility and reliability of rechargeable lithium/molybdenum disulfide batteries. *J. Power Sources* **25**, 265–276 (1989).
4. Fang, C., Wang, X. & Meng, Y. S. Key Issues Hindering a Practical Lithium-Metal Anode. *Trends Chem.* **1**, 152–158 (2019).
5. Jagger, B. & Pasta, M. Solid electrolyte interphases in lithium metal batteries. *Joule* **7**, 2228–2244 (2023).
6. He, X. *et al.* The passivity of lithium electrodes in liquid electrolytes for secondary batteries. *Nat. Rev. Mater.* **6**, 1036–1052 (2021).
7. Lu, D. *et al.* Failure Mechanism for Fast-Charged Lithium Metal Batteries with Liquid Electrolytes. *Adv. Energy Mater.* **5**, 1400993 (2015).
8. Wang, H. *et al.* Liquid electrolyte: The nexus of practical lithium metal batteries. *Joule* **6**, 588–616 (2022).
9. Boyle, D. T. *et al.* Correlating Kinetics to Cyclability Reveals Thermodynamic Origin of Lithium Anode Morphology in Liquid Electrolytes. *J. Am. Chem. Soc.* **144**, 20717–20725 (2022).
10. Yu, Z. *et al.* Rational solvent molecule tuning for high-performance lithium metal battery electrolytes. *Nat. Energy* **7**, 94–106 (2022).

11. Greatbatch, W. *et al.* The Solid-State Lithium Battery: A New Improved Chemical Power Source for Implantable Cardiac Pacemakers. *IEEE Trans. Biomed. Eng.* **BME-18**, 317–324 (1971).
12. Peled, E. The Electrochemical Behavior of Alkali and Alkaline Earth Metals in Nonaqueous Battery Systems—The Solid Electrolyte Interphase Model. *J. Electrochem. Soc.* **126**, 2047–2051 (1979).
13. Scarr, R. F. Kinetics of the Solid Lithium Electrode in Propylene Carbonate. *J. Electrochem. Soc.* **117**, 295 (1970).
14. Winter, M., Barnett, B. & Xu, K. Before Li Ion Batteries. *Chem. Rev.* **118**, 11433–11456 (2018).
15. Xu, K. Nonaqueous Liquid Electrolytes for Lithium-Based Rechargeable Batteries. *Chem. Rev.* **104**, 4303–4418 (2004).
16. Lewis, G. N. & Keyes, F. G. THE POTENTIAL OF THE LITHIUM ELECTRODE. *J. Am. Chem. Soc.* **35**, 340–344 (1913).
17. Harris, W. S. *ELECTROCHEMICAL STUDIES IN CYCLIC ESTERS*. UCRL--8381, 4305596 http://www.osti.gov/servlets/purl/4305596/ (1958) doi:10.2172/4305596.
18. Hirai, T., Yoshimatsu, I. & Yamaki, J. Effect of Additives on Lithium Cycling Efficiency. *J. Electrochem. Soc.* **141**, 2300–2305 (1994).
19. Xu, K. *Electrolytes, Interfaces and Interphases*. (The Royal Society of Chemistry, 2023). doi:10.1039/9781837671311.

20. Goodenough, J. B. & Kim, Y. Challenges for Rechargeable Li Batteries. *Chem. Mater.* **22**, 587–603 (2010).
21. Peljo, P. & Girault, H. H. Electrochemical potential window of battery electrolytes: the HOMO–LUMO misconception. *Energy Environ. Mater.* **11**, 2306 (2018).
22. Sethurajan, A. K., Krachkovskiy, S. A., Halalay, I. C., Goward, G. R. & Protas, B. Accurate Characterization of Ion Transport Properties in Binary Symmetric Electrolytes Using In Situ NMR Imaging and Inverse Modeling. *J Phys Chem B* **119**, 12238–48 (2015).
23. Hou, T. & Monroe, C. W. Composition-dependent thermodynamic and mass-transport characterization of lithium hexafluorophosphate in propylene carbonate. *Electrochimica Acta* **332**, (2020).
24. Wang, A. A., Hou, T., Karanjavala, M. & Monroe, C. W. Shifting-reference concentration cells to refine composition-dependent transport characterization of binary lithium-ion electrolytes. *Electrochimica Acta* **358**, (2020).
25. Diederichsen, K. M., McShane, E. J. & McCloskey, B. D. Promising Routes to a High Li+ Transference Number Electrolyte for Lithium Ion Batteries. *ACS Energy Lett.* **2**, 2563–2575 (2017).
26. Lorenz, M. *et al.* Local Volume Conservation in Concentrated Electrolytes Is Governing Charge Transport in Electric Fields. *J. Phys. Chem. Lett.* **13**, 8761–8767 (2022).

27. Schammer, M., Horstmann, B. & Latz, A. Theory of Transport in Highly Concentrated Electrolytes. *J. Electrochem. Soc.* **168**, 026511 (2021).
28. Petrowsky, M., Frech, R., Suarez, S. N., Jayakody, J. R. P. & Greenbaum, S. Investigation of Fundamental Transport Properties and Thermodynamics in Diglyme-Salt Solutions. *J. Phys. Chem. B* **110**, 23012–23021 (2006).
29. Wu, Q., McDowell, M. T. & Qi, Y. Effect of the Electric Double Layer (EDL) in Multicomponent Electrolyte Reduction and Solid Electrolyte Interphase (SEI) Formation in Lithium Batteries. *J. Am. Chem. Soc.* **145**, 2473–2484 (2023).
30. Angarita-Gomez, S. & Balbuena, P. B. Solvation *vs.* surface charge transfer: an interfacial chemistry game drives cation motion. *Chem. Commun.* **57**, 6189–6192 (2021).
31. Xu, K. Electrolytes and Interphases in Li-Ion Batteries and Beyond. *Chem. Rev.* **114**, 11503–11618 (2014).
32. Camacho-Forero, L. E., Smith, T. W. & Balbuena, P. B. Effects of High and Low Salt Concentration in Electrolytes at Lithium–Metal Anode Surfaces. *J. Phys. Chem. C* **121**, 182–194 (2017).
33. Qian, J. *et al.* High rate and stable cycling of lithium metal anode. *Nat. Commun.* **6**, 6362 (2015).
34. Sayah, S. *et al.* How do super concentrated electrolytes push the Li-ion batteries and supercapacitors beyond their thermodynamic and electrochemical limits? *Nano Energy* **98**, 107336 (2022).

35. Dokko, K. *et al.* Direct Evidence for Li Ion Hopping Conduction in Highly Concentrated Sulfolane-Based Liquid Electrolytes. *J. Phys. Chem. B* **122**, 10736–10745 (2018).
36. Chen, Y. *et al.* Steric Effect Tuned Ion Solvation Enabling Stable Cycling of High-Voltage Lithium Metal Battery. *J. Am. Chem. Soc.* **143**, 18703–18713 (2021).
37. Lin, Y.-X. *et al.* Connecting the irreversible capacity loss in Li-ion batteries with the electronic insulating properties of solid electrolyte interphase (SEI) components. *J. Power Sources* **309**, 221–230 (2016).
38. Li, Y. *et al.* Atomic structure of sensitive battery materials and interfaces revealed by cryo–electron microscopy. *Science* **358**, 506–510 (2017).
39. Xu, Y. *et al.* Atomic to Nanoscale Origin of Vinylene Carbonate Enhanced Cycling Stability of Lithium Metal Anode Revealed by Cryo-Transmission Electron Microscopy. *Nano Lett.* **20**, 418–425 (2020).
40. Wang, X. *et al.* New Insights on the Structure of Electrochemically Deposited Lithium Metal and Its Solid Electrolyte Interphases via Cryogenic TEM. *Nano Lett.* **17**, 7606–7612 (2017).
41. Zhang, Z. *et al.* Capturing the swelling of solid-electrolyte interphase in lithium metal batteries. *Science* **375**, 66–70 (2022).
42. Li, Y. & Qi, Y. Transferable Self-Consistent Charge Density Functional Tight-Binding Parameters for Li–Metal and Li-Ions in Inorganic Compounds and Organic Solvents. *J. Phys. Chem. C* **122**, 10755–10764 (2018).

43. Soto, F. A., Ma, Y., Martinez De La Hoz, J. M., Seminario, J. M. & Balbuena, P. B. Formation and Growth Mechanisms of Solid-Electrolyte Interphase Layers in Rechargeable Batteries. *Chem. Mater.* **27**, 7990–8000 (2015).
44. Single, F., Latz, A. & Horstmann, B. Identifying the Mechanism of Continued Growth of the Solid–Electrolyte Interphase. *ChemSusChem* **11**, 1950–1955 (2018).
45. Von Kolzenberg, L., Latz, A. & Horstmann, B. Solid–Electrolyte Interphase During Battery Cycling: Theory of Growth Regimes. *ChemSusChem* **13**, 3901–3910 (2020).
46. Single, F., Horstmann, B. & Latz, A. Dynamics and morphology of solid electrolyte interphase (SEI). *Phys. Chem. Chem. Phys.* **18**, 17810–17814 (2016).
47. Single, F., Horstmann, B. & Latz, A. Revealing SEI Morphology: In-Depth Analysis of a Modeling Approach. *J. Electrochem. Soc.* **164**, E3132–E3145 (2017).
48. Attia, P. M., Das, S., Harris, S. J., Bazant, M. Z. & Chueh, W. C. Electrochemical Kinetics of SEI Growth on Carbon Black: Part I. Experiments. *J. Electrochem. Soc.* **166**, E97–E106 (2019).
49. Harris, O. C., Lin, Y., Qi, Y., Leung, K. & Tang, M. H. How Transition Metals Enable Electron Transfer through the SEI: Part I. Experiments and Butler-Volmer Modeling. *J. Electrochem. Soc.* **167**, 013502 (2020).

50. Menkin, S. *et al.* Toward an Understanding of SEI Formation and Lithium Plating on Copper in Anode-Free Batteries. *J. Phys. Chem. C* **125**, 16719–16732 (2021).
51. Wang, H. *et al.* The effect of removing the native passivation film on the electrochemical performance of lithium metal electrodes. *J. Power Sources* **520**, 230817 (2022).
52. Kühn, S. P. *et al.* Back to the basics: Advanced understanding of the as-defined solid electrolyte interphase on lithium metal electrodes. *J. Power Sources* **549**, 232118 (2022).
53. Otto, S.-K. *et al.* Storage of Lithium Metal: The Role of the Native Passivation Layer for the Anode Interface Resistance in Solid State Batteries. *ACS Appl. Energy Mater.* **4**, 12798–12807 (2021).
54. Zhou, B., Bonakdarpour, A., Stoševski, I., Fang, B. & Wilkinson, D. P. Modification of Cu current collectors for lithium metal batteries – A review. *Prog. Mater. Sci.* **130**, 100996 (2022).
55. Yoon, J. S. *et al.* Thermodynamics, Adhesion, and Wetting at Li/Cu(-Oxide) Interfaces: Relevance for Anode-Free Lithium–Metal Batteries. *ACS Appl. Mater. Interfaces* **16**, 18790–18799 (2024).
56. Aravindan, V., Gnanaraj, J., Madhavi, S. & Liu, H. Lithium-Ion Conducting Electrolyte Salts for Lithium Batteries. *Chem. – Eur. J.* **17**, 14326–14346 (2011).
57. Schmitz, R. W. *et al.* Investigations on novel electrolytes, solvents and SEI additives for use in lithium-ion batteries: Systematic electrochemical

characterization and detailed analysis by spectroscopic methods. *Prog. Solid State Chem.* **42**, 65–84 (2014).

58. Yeddala, M., Rynearson, L. & Lucht, B. L. Modification of Carbonate Electrolytes for Lithium Metal Electrodes. *ACS Energy Lett.* **8**, 4782–4793 (2023).
59. Kwon, Y. *et al.* Elucidating the role of cathode identity: Voltage-dependent reversibility of anode-free batteries. *Chem* **10**, 3159–3183 (2024).
60. Ishikawa, M., Tasaka, Y., Yoshimoto, N. & Morita, M. Optimization of physicochemical characteristics of a lithium anode interface for high-efficiency cycling: an effect of electrolyte temperature. *J. Power Sources* **97–98**, 262–264 (2001).
61. Wang, J. *et al.* Improving cyclability of Li metal batteries at elevated temperatures and its origin revealed by cryo-electron microscopy. *Nat. Energy* **4**, 664–670 (2019).
62. Peled, E. & Menkin, S. Review—SEI: Past, Present and Future. *J. Electrochem. Soc.* **164**, A1703–A1719 (2017).
63. McBrayer, J. D., Apblett, C. A., Harrison, K. L., Fenton, K. R. & Minteer, S. D. Mechanical studies of the solid electrolyte interphase on anodes in lithium and lithium ion batteries. *Nanotechnology* **32**, 502005 (2021).
64. Yuan, S. *et al.* Revisiting the designing criteria of advanced solid electrolyte interphase on lithium metal anode under practical condition. *Nano Energy* **83**, 105847 (2021).

65. Shen, X. *et al.* The Failure of Solid Electrolyte Interphase on Li Metal Anode: Structural Uniformity or Mechanical Strength? *Adv. Energy Mater.* **10**, 1903645 (2020).
66. Monroe, C. & Newman, J. The Impact of Elastic Deformation on Deposition Kinetics at Lithium/Polymer Interfaces. *J. Electrochem. Soc.* **152**, A396 (2005).
67. Gao, Y. *et al.* Unraveling the mechanical origin of stable solid electrolyte interphase. *Joule* **5**, 1860–1872 (2021).
68. Gu, Y. *et al.* Designable ultra-smooth ultra-thin solid-electrolyte interphases of three alkali metal anodes. *Nat. Commun.* **9**, 1339 (2018).
69. Wang, J. *et al.* In Situ Self-Assembly of Ordered Organic/Inorganic Dual-Layered Interphase for Achieving Long-Life Dendrite-Free Li Metal Anodes in LiFSI-Based Electrolyte. *Adv. Funct. Mater.* **31**, 2007434 (2021).
70. Shi, S. *et al.* Direct Calculation of Li-Ion Transport in the Solid Electrolyte Interphase. *J. Am. Chem. Soc.* **134**, 15476–15487 (2012).
71. Lu, P. & Harris, S. J. Lithium transport within the solid electrolyte interphase. *Electrochem. Commun.* **13**, 1035–1037 (2011).
72. Yu, X. *et al.* Direct and in situ examination of Li+ transport kinetics in isotope labelled solid electrolyte interphase. Preprint at https://doi.org/10.48550/ARXIV.2308.04701 (2023).
73. Das Goswami, B. R., Jabbari, V., Shahbazian-Yassar, R., Mashayek, F. & Yurkiv, V. Unraveling Ion Diffusion Pathways and Energetics in Polycrystalline SEI of

Lithium-Based Batteries: Combined Cryo-HRTEM and DFT Study. *J. Phys. Chem. C* **127**, 21971–21979 (2023).

74. Soto, F. A., Marzouk, A., El-Mellouhi, F. & Balbuena, P. B. Understanding Ionic Diffusion through SEI Components for Lithium-Ion and Sodium-Ion Batteries: Insights from First-Principles Calculations. *Chem. Mater.* **30**, 3315–3322 (2018).
75. Xu, Y. *et al.* Direct in situ measurements of electrical properties of solid–electrolyte interphase on lithium metal anodes. *Nat. Energy* **8**, 1345–1354 (2023).
76. Benitez, L. & Seminario, J. M. Electron Transport and Electrolyte Reduction in the Solid-Electrolyte Interphase of Rechargeable Lithium Ion Batteries with Silicon Anodes. *J. Phys. Chem. C* **120**, 17978–17988 (2016).
77. Derosa, P. A. & Seminario, J. M. Electron Transport through Single Molecules: Scattering Treatment Using Density Functional and Green Function Theories. *J. Phys. Chem. B* **105**, 471–481 (2001).
78. Köbbing, L., Latz, A. & Horstmann, B. Growth of the solid-electrolyte interphase: Electron diffusion versus solvent diffusion. *J. Power Sources* **561**, 232651 (2023).
79. Feng, M., Pan, J. & Qi, Y. Impact of Electronic Properties of Grain Boundaries on the Solid Electrolyte Interphases (SEIs) in Li-ion Batteries. *J. Phys. Chem. C* **125**, 15821–15829 (2021).
80. Fang, C. *et al.* Quantifying inactive lithium in lithium metal batteries. *Nature* **572**, 511–515 (2019).

81. Werres, M. *et al.* Origin of Heterogeneous Stripping of Lithium in Liquid Electrolytes. *ACS Nano* **17**, 10218–10228 (2023).
82. Bai, P., Li, J., Brushett, F. R. & Bazant, M. Z. Transition of lithium growth mechanisms in liquid electrolytes. *Energy Environ. Sci.* **9**, 3221–3229 (2016).
83. Steiger, J., Kramer, D. & Mönig, R. Mechanisms of dendritic growth investigated by in situ light microscopy during electrodeposition and dissolution of lithium. *J. Power Sources* **261**, 112–119 (2014).
84. Xu, Y. *et al.* Current Density Regulated Atomic to Nanoscale Process on Li Deposition and Solid Electrolyte Interphase Revealed by Cryogenic Transmission Electron Microscopy. *ACS Nano* **14**, 8766–8775 (2020).
85. Boyle, D. T. *et al.* Resolving Current-Dependent Regimes of Electroplating Mechanisms for Fast Charging Lithium Metal Anodes. *Nano Lett.* **22**, 8224–8232 (2022).
86. He, M., Guo, R., Hobold, G. M., Gao, H. & Gallant, B. M. The intrinsic behavior of lithium fluoride in solid electrolyte interphases on lithium. *Proc. Natl. Acad. Sci.* **117**, 73–79 (2020).
87. Zhang, X.-Q., Cheng, X.-B., Chen, X., Yan, C. & Zhang, Q. Fluoroethylene Carbonate Additives to Render Uniform Li Deposits in Lithium Metal Batteries. *Adv. Funct. Mater.* **27**, 1605989 (2017).
88. Dhattarwal, H. S., Kuo, J.-L. & Kashyap, H. K. Mechanistic Insight on the Stability of Ether and Fluorinated Ether Solvent-Based Lithium

Bis(fluoromethanesulfonyl) Electrolytes near Li Metal Surface. *J. Phys. Chem. C* **126**, 8953–8963 (2022).

89. Perez-Beltran, S., Kuai, D. & Balbuena, P. B. SEI Formation and Lithium-Ion Electrodeposition Dynamics in Lithium Metal Batteries via First-Principles Kinetic Monte Carlo Modeling. *ACS Energy Lett.* **9**, 5268–5278 (2024).
90. Tan, Y. *et al.* Lithium Fluoride in Electrolyte for Stable and Safe Lithium-Metal Batteries. *Adv. Mater.* **33**, 2102134 (2021).
91. Zeng, H. *et al.* Beyond LiF: Tailoring Li_2 O-Dominated Solid Electrolyte Interphase for Stable Lithium Metal Batteries. *ACS Nano* **18**, 1969–1981 (2024).
92. Hobold, G. M., Wang, C., Steinberg, K., Li, Y. & Gallant, B. M. High lithium oxide prevalence in the lithium solid–electrolyte interphase for high Coulombic efficiency. *Nat. Energy* **9**, 580–591 (2024).
93. Borodin, O., Self, J., Persson, K. A., Wang, C. & Xu, K. Uncharted Waters: Super-Concentrated Electrolytes. *Joule* **4**, 69–100 (2020).
94. Jiang, G. *et al.* Perspective on High-Concentration Electrolytes for Lithium Metal Batteries. *Small Struct.* **2**, 2000122 (2021).
95. Ren, X. *et al.* Enabling High-Voltage Lithium-Metal Batteries under Practical Conditions. *Joule* **3**, 1662–1676 (2019).
96. Ren, X. *et al.* Localized High-Concentration Sulfone Electrolytes for High-Efficiency Lithium-Metal Batteries. *Chem* **4**, 1877–1892 (2018).

97. Zheng, J. *et al.* Extremely Stable Sodium Metal Batteries Enabled by Localized High-Concentration Electrolytes. *ACS Energy Lett.* **3**, 315–321 (2018).

98. Efaw, C. M. *et al.* Localized high-concentration electrolytes get more localized through micelle-like structures. *Nat. Mater.* **22**, 1531–1539 (2023).

99. Verma, A., Schulze, M. C. & Colclasure, A. Micelle-like bulk structure of localized high-concentration electrolytes. *Joule* **8**, 10–12 (2024).

100. Cao, X., Jia, H., Xu, W. & Zhang, J.-G. Review—Localized High-Concentration Electrolytes for Lithium Batteries. *J. Electrochem. Soc.* **168**, 010522 (2021).

101. Chen, J. *et al.* Design of Localized High-Concentration Electrolytes via Donor Number. *ACS Energy Lett.* **8**, 1723–1734 (2023).

102. Ren, F. *et al.* Solvent–Diluent Interaction-Mediated Solvation Structure of Localized High-Concentration Electrolytes. *ACS Appl. Mater. Interfaces* **14**, 4211–4219 (2022).

103. Chen, S. *et al.* High-Voltage Lithium-Metal Batteries Enabled by Localized High-Concentration Electrolytes. *Adv. Mater.* **30**, 1706102 (2018).

104. Zhang, X. *et al.* Advanced Electrolytes for Fast-Charging High-Voltage Lithium-Ion Batteries in Wide-Temperature Range. *Adv. Energy Mater.* **10**, 2000368 (2020).

105. Jia, H. *et al.* High-Performance Silicon Anodes Enabled By Nonflammable Localized High-Concentration Electrolytes. *Adv. Energy Mater.* **9**, 1900784 (2019).

106. Ahmed, R. A. *et al.* Enhanced Electrochemical Performance of Disordered Rocksalt Cathodes in a Localized High-Concentration Electrolyte. *Adv. Energy Mater.* **14**, 2400722 (2024).

107. Cao, X. *et al.* Optimization of fluorinated orthoformate based electrolytes for practical high-voltage lithium metal batteries. *Energy Storage Mater.* **34**, 76–84 (2021).

108. Cao, X. *et al.* Effects of fluorinated solvents on electrolyte solvation structures and electrode/electrolyte interphases for lithium metal batteries. *Proc. Natl. Acad. Sci.* **118**, (2021).

109. Niu, C. *et al.* High-energy lithium metal pouch cells with limited anode swelling and long stable cycles. *Nat. Energy* **4**, 551–559 (2019).

110. Perez Beltran, S., Cao, X., Zhang, J.-G., El-Khoury, P. Z. & Balbuena, P. B. Influence of diluent concentration in localized high concentration electrolytes: elucidation of hidden diluent-Li^+ interactions and Li^+ transport mechanism. *J. Mater. Chem. A* **9**, 17459–17473 (2021).

111. Liu, Y. *et al.* Regulating Electrolyte Solvation Structures via Diluent-Solvent Interactions for Safe High-Voltage Lithium Metal Batteries. *Small* **20**, 2311812 (2024).

112. Zhao, Y. *et al.* Electrolyte engineering for highly inorganic solid electrolyte interphase in high-performance lithium metal batteries. *Chem* **9**, 682–697 (2023).

113. Shi, J. *et al.* An Amphiphilic Molecule-Regulated Core-Shell-Solvation Electrolyte for Li-Metal Batteries at Ultra-Low Temperature. *Angew. Chem. Int. Ed.* **62**, e202218151 (2023).

114. Kim, S. *et al.* Wide-temperature-range operation of lithium-metal batteries using partially and weakly solvating liquid electrolytes. *Energy Environ. Sci.* **16**, 5108–5122 (2023).

115. Tran, T. *et al.* Enhancing Cycling Stability of Lithium Metal Batteries by a Bifunctional Fluorinated Ether. *Adv. Funct. Mater.* 2407012 (2024) doi:10.1002/adfm.202407012.

116. Hai, F. *et al.* A Low-Cost, Fluorine-Free Localized Highly Concentrated Electrolyte Toward Ultra-High Loading Lithium Metal Batteries. *Adv. Energy Mater.* **14**, 2304253 (2024).

117. Yuan, Z., Chen, A., Liao, J., Song, L. & Zhou, X. Recent advances in multifunctional generalized local high-concentration electrolytes for high-efficiency alkali metal batteries. *Nano Energy* **119**, 109088 (2024).

118. Li, M. *et al.* Acetonitrile-Based Local High-Concentration Electrolytes for Advanced Lithium Metal Batteries. *Adv. Mater.* 2404271 (2024) doi:10.1002/adma.202404271.

119. Jie, Y. *et al.* Towards long-life 500 Wh kg-1 lithium metal pouch cells via compact ion-pair aggregate electrolytes. *Nat. Energy* **9**, 987–998 (2024).

120. Kim, S. C. *et al.* High-entropy electrolytes for practical lithium metal batteries. *Nat. Energy* **8**, 814–826 (2023).

121. Li, Z. *et al.* Critical Review of Fluorinated Electrolytes for High-Performance Lithium Metal Batteries. *Adv. Funct. Mater.* **33**, 2300502 (2023).

122. Yeddala, M., Rynearson, L. & Lucht, B. L. Modification of Carbonate Electrolytes for Lithium Metal Electrodes. *ACS Energy Lett.* **8**, 4782–4793 (2023).

123. Markevich, E., Salitra, G., Chesneau, F., Schmidt, M. & Aurbach, D. Very Stable Lithium Metal Stripping–Plating at a High Rate and High Areal Capacity in Fluoroethylene Carbonate-Based Organic Electrolyte Solution. *ACS Energy Lett.* **2**, 1321–1326 (2017).

124. Brown, Z. L., Jurng, S., Nguyen, C. C. & Lucht, B. L. Effect of Fluoroethylene Carbonate Electrolytes on the Nanostructure of the Solid Electrolyte Interphase and Performance of Lithium Metal Anodes. *ACS Appl. Energy Mater.* **1**, 3057–3062 (2018).

125. Yu, Z. *et al.* Molecular design for electrolyte solvents enabling energy-dense and long-cycling lithium metal batteries. *Nat. Energy* **5**, 526–533 (2020).

126. Zhang, G. *et al.* A monofluoride ether-based electrolyte solution for fast-charging and low-temperature non-aqueous lithium metal batteries. *Nat. Commun.* **14**, 1081 (2023).

127. Xue, W. *et al.* FSI-inspired solvent and “full fluorosulfonyl” electrolyte for 4 V class lithium-metal batteries. *Energy Environ. Sci.* **13**, 212–220 (2020).

128. Xue, W. *et al.* Ultra-high-voltage Ni-rich layered cathodes in practical Li metal batteries enabled by a sulfonamide-based electrolyte. *Nat. Energy* **6**, 495–505 (2021).

129. Feng, S. *et al.* Molecular Design of Stable Sulfamide- and Sulfonamide-Based Electrolytes for Aprotic Li-O2 Batteries. *Chem* **5**, 2630–2641 (2019).

130. Rustomji, C. S. *et al.* Liquefied gas electrolytes for electrochemical energy storage devices. *Science* **356**, eaal4263 (2017).

131. Yang, Y. *et al.* High-Efficiency Lithium-Metal Anode Enabled by Liquefied Gas Electrolytes. *Joule* **3**, 1986–2000 (2019).

132. Vu, M. C. *et al.* Low melting alkali-based molten salt electrolytes for solvent-free lithium-metal batteries. *Matter* **6**, 4357–4375 (2023).

133. Louli, A. J. *et al.* Diagnosing and correcting anode-free cell failure via electrolyte and morphological analysis. *Nat. Energy* **5**, 693–702 (2020).

134. Weber, R. *et al.* Long cycle life and dendrite-free lithium morphology in anode-free lithium pouch cells enabled by a dual-salt liquid electrolyte. *Nat. Energy* **4**, 683–689 (2019).

135. Qiu, F. *et al.* A Concentrated Ternary-Salts Electrolyte for High Reversible Li Metal Battery with Slight Excess Li. *Adv. Energy Mater.* **9**, 1803372 (2019).

136. Kang, D. W., Moon, J., Choi, H.-Y., Shin, H.-C. & Kim, B. G. Stable cycling and uniform lithium deposition in anode-free lithium-metal batteries enabled by a high-concentration dual-salt electrolyte with high LiNO3 content. *J. Power Sources* **490**, 229504 (2021).

137. Beyene, T. T. *et al.* Concentrated Dual-Salt Electrolyte to Stabilize Li Metal and Increase Cycle Life of Anode Free Li-Metal Batteries. *J. Electrochem. Soc.* **166**, A1501–A1509 (2019).

138. Ma, Q. *et al.* Improved Cycling Stability of Lithium-Metal Anode with Concentrated Electrolytes Based on Lithium (Fluorosulfonyl) (trifluoromethanesulfonyl)imide. *ChemElectroChem* **3**, 531–536 (2016).

139. Weintz, D., Kühn, S. P., Winter, M. & Cekic-Laskovic, I. Tailoring the Preformed Solid Electrolyte Interphase in Lithium Metal Batteries: Impact of Fluoroethylene Carbonate. *ACS Appl. Mater. Interfaces* **15**, 53526–53532 (2023).

140. Xue, T. *et al.* Tailoring fluorine-rich solid electrolyte interphase to boost high efficiency and long cycling stability of lithium metal batteries. *Sci. China Chem.* **66**, 2121–2129 (2023).

141. Stuckenberg, S. *et al.* Influence of $LiNO_3$ on the Lithium Metal Deposition Behavior in Carbonate-Based Liquid Electrolytes and on the Electrochemical Performance in Zero-Excess Lithium Metal Batteries. *Small* **20**, 2305203 (2024).

142. Ding, F. *et al.* Dendrite-Free Lithium Deposition via Self-Healing Electrostatic Shield Mechanism. *J. Am. Chem. Soc.* **135**, 4450–4456 (2013).

143. Morita, M., Asai, Y., Yoshimoto, N. & Ishikawa, M. A Raman spectroscopic study of organic electrolyte solutions based on binary solvent systems of ethylene carbonate with low viscosity solvents which dissolve different lithium salts. *J. Chem. Soc. Faraday Trans.* **94**, 3451–3456 (1998).

144. Qian, K., Winans, R. E. & Li, T. Insights into the Nanostructure, Solvation, and Dynamics of Liquid Electrolytes through Small-Angle X-Ray Scattering. *Adv. Energy Mater.* **11**, 2002821 (2021).

145. Single, F., Horstmann, B. & Latz, A. Theory of Impedance Spectroscopy for Lithium Batteries. *J. Phys. Chem. C* **123**, 27327–27343 (2019).

146. Leifer, N., Aurbach, D. & Greenbaum, S. G. NMR studies of lithium and sodium battery electrolytes. *Prog. Nucl. Magn. Reson. Spectrosc.* **142–143**, 1–54 (2024).

147. Bergstrom, H. K. & McCloskey, B. D. Ion Transport in (Localized) High Concentration Electrolytes for Li-Based Batteries. *ACS Energy Lett.* **9**, 373–380 (2024).

148. Zugmann, S. *et al.* Measurement of transference numbers for lithium ion electrolytes via four different methods, a comparative study. *Electrochimica Acta* **56**, 3926–3933 (2011).

149. Kim, T. *et al.* Applications of Voltammetry in Lithium Ion Battery Research. *J. Electrochem. Sci. Technol.* **11**, 14–25 (2020).

150. Hess, S., Wohlfahrt-Mehrens, M. & Wachtler, M. Flammability of Li-Ion Battery Electrolytes: Flash Point and Self-Extinguishing Time Measurements. *J. Electrochem. Soc.* **162**, A3084–A3097 (2015).

151. Hellweg, L., Beuse, T., Winter, M. & Börner, M. Influence of Lithium Metal Deposition on Thermal Stability: Combined DSC and Morphology Analysis of Cyclic Aged Lithium Metal Batteries. *J. Electrochem. Soc.* **170**, 040530 (2023).

152. Arbizzani, C., Gabrielli, G. & Mastragostino, M. Thermal stability and flammability of electrolytes for lithium-ion batteries. *J. Power Sources* **196**, 4801–4805 (2011).

153. Adams, B. D., Zheng, J., Ren, X., Xu, W. & Zhang, J. Accurate Determination of Coulombic Efficiency for Lithium Metal Anodes and Lithium Metal Batteries. *Adv. Energy Mater.* **8**, 1702097 (2018).

154. Meunier, V., Leal De Souza, M., Morcrette, M. & Grimaud, A. Design of workflows for crosstalk detection and lifetime deviation onset in Li-ion batteries. *Joule* **7**, 42–56 (2023).

155. Meng, W. *et al.* The progress of *in situ* technology for lithium metal batteries. *Mater. Chem. Front.* **8**, 700–714 (2024).

156. Cao, X. *et al.* Monolithic solid–electrolyte interphases formed in fluorinated orthoformate-based electrolytes minimize Li depletion and pulverization. *Nat. Energy* **4**, 796–805 (2019).

157. Wang, J. *et al.* Improving cyclability of Li metal batteries at elevated temperatures and its origin revealed by cryo-electron microscopy. *Nat. Energy* **4**, 664–670 (2019).

158. Gao, Y. *et al.* Low-temperature and high-rate-charging lithium metal batteries enabled by an electrochemically active monolayer-regulated interface. *Nat. Energy* **5**, 534–542 (2020).

159. Liu, Z. *et al.* Interfacial Study on Solid Electrolyte Interphase at Li Metal Anode: Implication for Li Dendrite Growth. *J. Electrochem. Soc.* **163**, A592–A598 (2016).

160. Smeu, M. & Leung, K. Electron leakage through heterogeneous LiF on lithium–metal battery anodes. *Phys. Chem. Chem. Phys.* **23**, 3214–3218 (2021).

161. Wang, L. *et al.* In-situ visualization of the space-charge-layer effect on interfacial lithium-ion transport in all-solid-state batteries. *Nat. Commun.* **11**, 5889 (2020).

162. Chen, W. *et al.* Formation and impact of nanoscopic oriented phase domains in electrochemical crystalline electrodes. *Nat. Mater.* **22**, 92–99 (2023).

163. Zhang, Z. *et al.* Characterizing Batteries by In Situ Electrochemical Atomic Force Microscopy: A Critical Review. *Adv. Energy Mater.* **11**, 2101518 (2021).

164. Lang, S.-Y. & Wen, R. Understanding the solid electrolyte interphases in battery systems by electrochemical atomic force microscopy and its derivatives. *Curr. Opin. Electrochem.* **46**, 101523 (2024).

165. Wolff, B. & Hausen, F. Mechanical Evolution of Solid Electrolyte Interphase on Metallic Lithium Studied by in situ Atomic Force Microscopy. *J. Electrochem. Soc.* **170**, 010534 (2023).

166. Zhang, H., Shen, C., Huang, Y. & Liu, Z. Spontaneously formation of SEI layers on lithium metal from LiFSI/DME and LiTFSI/DME electrolytes. *Appl. Surf. Sci.* **537**, 147983 (2021).

167. Shadike, Z. *et al.* Identification of LiH and nanocrystalline LiF in the solid-electrolyte interphase of lithium metal anodes. *Nat. Nanotechnol.* **16**, 549–554 (2021).

168. Tan, S. *et al.* Evolution and Interplay of Lithium Metal Interphase Components Revealed by Experimental and Theoretical Studies. *J. Am. Chem. Soc.* **146**, 11711–11718 (2024).

169. Ma, C., Xu, F. & Song, T. Dual-Layered Interfacial Evolution of Lithium Metal Anode: SEI Analysis via TOF-SIMS Technology. *ACS Appl. Mater. Interfaces* **14**, 20197–20207 (2022).

170. Markevich, E., Salitra, G., Chesneau, F., Schmidt, M. & Aurbach, D. Very Stable Lithium Metal Stripping–Plating at a High Rate and High Areal Capacity in Fluoroethylene Carbonate-Based Organic Electrolyte Solution. *ACS Energy Lett.* **2**, 1321–1326 (2017).

171. Schmitz, R. *et al.* SEI investigations on copper electrodes after lithium plating with Raman spectroscopy and mass spectrometry. *J. Power Sources* **233**, 110–114 (2013).

172. Hope, M. A. *et al.* Selective NMR observation of the SEI–metal interface by dynamic nuclear polarisation from lithium metal. *Nat. Commun.* **11**, 2224 (2020).

173. Hsieh, Y.-C. *et al.* Quantification of Dead Lithium via In Situ Nuclear Magnetic Resonance Spectroscopy. *Cell Rep. Phys. Sci.* **1**, 100139 (2020).

174. Gunnarsdóttir, A. B., Vema, S., Menkin, S., Marbella, L. E. & Grey, C. P. Investigating the effect of a fluoroethylene carbonate additive on lithium deposition and the solid electrolyte interphase in lithium metal batteries using *in situ* NMR spectroscopy. *J. Mater. Chem. A* **8**, 14975–14992 (2020).

175. Fang, C. *et al.* Large-Molecule Decomposition Products of Electrolytes and Additives Revealed by On-Electrode Chromatography and MALDI. *Joule* **5**, 415–428 (2021).

176. Golozar, M. *et al.* In situ observation of solid electrolyte interphase evolution in a lithium metal battery. *Commun. Chem.* **2**, 131 (2019).

177. He, Y. *et al.* Progressive growth of the solid–electrolyte interphase towards the Si anode interior causes capacity fading. *Nat. Nanotechnol.* **16**, 1113–1120 (2021).

178. Zachman, M. J., Tu, Z., Choudhury, S., Archer, L. A. & Kourkoutis, L. F. Cryo-STEM mapping of solid–liquid interfaces and dendrites in lithium-metal batteries. *Nature* **560**, 345–349 (2018).

179. He, X., Larson, J. M., Bechtel, H. A. & Kostecki, R. In situ infrared nanospectroscopy of the local processes at the Li/polymer electrolyte interface. *Nat. Commun.* **13**, 1398 (2022).

180. Dopilka, A., Gu, Y., Larson, J. M., Zorba, V. & Kostecki, R. Nano-FTIR Spectroscopy of the Solid Electrolyte Interphase Layer on a Thin-Film Silicon Li-Ion Anode. *ACS Appl. Mater. Interfaces* **15**, 6755–6767 (2023).

181. Perez Beltran, S. & Balbuena, P. B. SEI formation mechanisms and Li+ dissolution in lithium metal anodes: Impact of the electrolyte composition and the electrolyte-to-anode ratio. *J. Power Sources* **551**, 232203 (2022).

182. Wagner-Henke, J. *et al.* Knowledge-driven design of solid-electrolyte interphases on lithium metal via multiscale modelling. *Nat. Commun.* **14**, 6823 (2023).

183. Benayad, A. *et al.* High-Throughput Experimentation and Computational Freeway Lanes for Accelerated Battery Electrolyte and Interface Development Research. *Adv. Energy Mater.* **12**, 2102678 (2022).

184. Ward, L. *et al.* Principles of the Battery Data Genome. *Joule* **6**, 2253–2271 (2022).

185. Qu, X. *et al.* The Electrolyte Genome project: A big data approach in battery materials discovery. *Comput. Mater. Sci.* **103**, 56–67 (2015).

186. Tagade, P. M. *et al.* Attribute driven inverse materials design using deep learning Bayesian framework. *Npj Comput. Mater.* **5**, 127 (2019).

187. Barter, D. *et al.* Predictive stochastic analysis of massive filter-based electrochemical reaction networks. *Digit. Discov.* **2**, 123–137 (2023).

188. Gao, Y.-C. *et al.* Data-Driven Insight into the Reductive Stability of Ion–Solvent Complexes in Lithium Battery Electrolytes. *J. Am. Chem. Soc.* **145**, 23764–23770 (2023).

189. Cheng, L. *et al.* Accelerating Electrolyte Discovery for Energy Storage with High-Throughput Screening. *J. Phys. Chem. Lett.* **6**, 283–291 (2015).

190. Matsuda, S., Nishioka, K. & Nakanishi, S. High-throughput combinatorial screening of multi-component electrolyte additives to improve the performance of Li metal secondary batteries. *Sci. Rep.* **9**, 6211 (2019).

191. Yan, P. *et al.* Non-aqueous battery electrolytes: high-throughput experimentation and machine learning-aided optimization of ionic conductivity. *J. Mater. Chem. A* 10.1039.D3TA06249J (2024) doi:10.1039/D3TA06249J.

192. Dave, A. *et al.* Autonomous optimization of non-aqueous Li-ion battery electrolytes via robotic experimentation and machine learning coupling. *Nat. Commun.* **13**, 5454 (2022).

193. Flores, E. *et al.* Learning the laws of lithium-ion transport in electrolytes using symbolic regression. *Digit. Discov.* **1**, 440–447 (2022).

194. Rahmanian, F. *et al.* One-Shot Active Learning for Globally Optimal Battery Electrolyte Conductivity**. *Batter. Supercaps* **5**, e202200228 (2022).